

**Supplementary Data**

**Tailored Magnetic Properties in CoFeB-BiFeO<sub>3</sub> Nanocomposite Thin Films**

Lizabeth Quigley,<sup>1</sup> Nirali A. Bhatt,<sup>1</sup> Katrina Evancho,<sup>1</sup> Jianan Shen,<sup>1</sup> Juanjuan Lu,<sup>1</sup> Claire A. Mihalko,<sup>1</sup> James P. Barnard,<sup>1</sup> Max Chhabra,<sup>1</sup> Ping Lu,<sup>2,3</sup> Raktim Sarma,<sup>2,3</sup> Aleem Siddiqui,<sup>2</sup> Haiyan Wang<sup>1, 4\*</sup>

<sup>1</sup> School of Materials Engineering, Purdue University, West Lafayette, Indiana 47907, USA

<sup>2</sup> Sandia National Laboratories, Albuquerque, New Mexico 87185, USA

<sup>3</sup> Center for Integrated Nanotechnologies, Sandia National Laboratories, Albuquerque, New Mexico 87185, USA

<sup>4</sup> School of Electrical and Computer Engineering, Purdue University, West Lafayette, Indiana 47907, USA

\*Corresponding Author: [hwang00@purdue.edu](mailto:hwang00@purdue.edu)

The Supporting Information contains the following Figures and Tables:

**Figure S1:** Phi scans of A) Nitrogen PiM film, B) Vacuum PiM film, and C) Bilayer Film centered on the 1) CFB (100) plane and 2) STO (110) plane. The black line in the CFB (100) graphs represents a smoothed fit of the data to get an overall representation of it.

**Figure S2:** XRD  $\theta$ - $2\theta$  of the A) Pure CFB film and B) Pure BFO film.

**Figure S3:** For the Pure BFO film: A1) Low-magnification, A2) Medium-magnification, and A3) High-magnification TEM images, A4) STEM image for the corresponding EDS maps, EDS maps of the following elements A5) Bi- and Ti-, A6) Bi-, Fe-, and Ti-, A7) Bi-, A8) Fe-, and A9) O-. For the Pure CFB film: A1) Low-magnification, A2) Medium-magnification, and A3) High-magnification TEM images, A4) STEM image for the corresponding EDS maps, EDS maps of the following elements A5) Co- and Ti-, A6) Co-, Fe-, and Ti-, A7) Bi-, A8) Fe-, and A9) O-.

**Figure S4:** Magnetic hysteresis (MvsH) data showing both in-plane (IP) and out-of-plane (OP) orientations for the Pure BFO and Pure CFB films at A) 300 K and B) 10 K.

**Figure S5:** For the Nitrogen PiM film: A1) Schematic drawing, A2) Medium-magnification TEM image, A3) STEM image for corresponding EDS maps, EDS maps of the following elements A4) Co-, Bi-, Fe-, and Ti-, A5) Co-, A6) Bi-, A7) O-, and A8) Fe-. For the Vacuum PiM film: B1) Schematic drawing, B2) Medium-magnification TEM image, B3) STEM image for corresponding EDS maps, EDS maps of the following elements B4) Co-, Bi-, Fe-, and Ti-, B5) Co-, B6) Bi-, B7) O-, and B8) Fe-. For the Bilayer film: C1) Schematic drawing, C2) Medium-magnification TEM image, C3) STEM image for corresponding EDS maps, EDS maps of the following elements C4) Co-, Bi-, Fe-, and Ti-, C5) Co-, C6) Bi-, C7) O-, and C8) Fe-.

**Table S1:** List of Film Thicknesses

**Table S2:** List of the Saturation Magnetization and Coercivity for all the samples.

**Figure S6:** Magnetic hysteresis ( $M$  vs.  $H$ ) data showing the out-of-plane data at 10 K after Zero-Field Cooling, Positive Field Cooling, and Negative Field Cooling for the A) Nitrogen PiM film, B) Vacuum PiM film, and C) Bilayer Film. D) Normalized Zero Field-Cooled (ZFC) and Field-Cooled (FC) for the Nitrogen PiM, Vacuum PiM, and Bilayer films. The measurement was done with an applied field of 1000 Oe, and the normalization was done individually for each sample.

**Table S3:** List of the Coercive Field,  $H_C$ , (kOe) and Exchange Bias Field,  $H_{EB}$ , (kOe) of the Nitrogen PiM, Vacuum PiM, and Bilayer films after cooling to 10 K under Zero-Field, Positive Field, and Negative Field.

**Figure S7:** Electrical hysteresis ( $P$  vs.  $E$  data) for the A) Nitrogen PiM, B) Vacuum PiM, and C) Bilayer films.

**Figure S8:** Electrical hysteresis ( $P$  vs.  $E$ ) data for the Nitrogen PiM sample at A1) First measured spot, A2) Second measured spot, for the Vacuum PiM film B1) First measured spot, B2) Second measured spot, and for the Bilayer film C1) First measured spot, C2) Second measured spot.

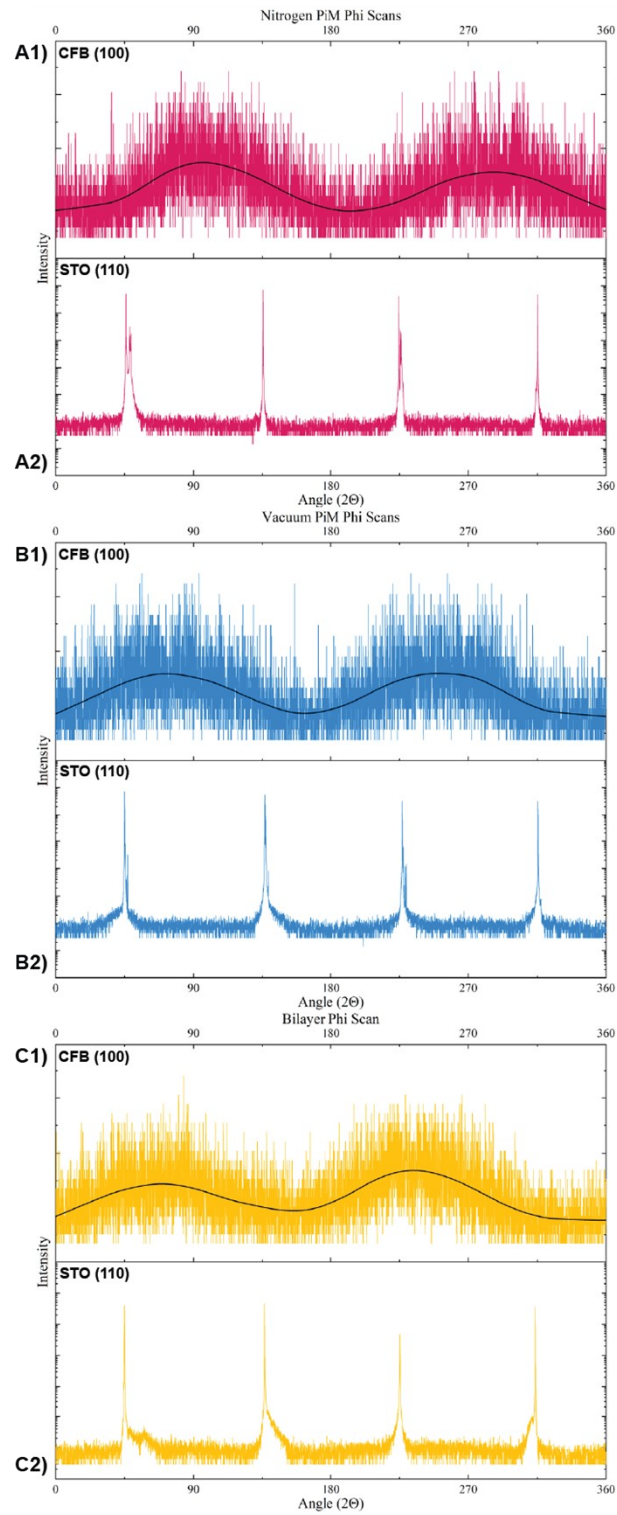


Figure S1: Phi scans of A) Nitrogen PiM film, B) Vacuum PiM film, and C) Bilayer Film centered on the 1) CFB (100) plane and 2) STO (110) plane. The black line in the CFB (100) graphs represents a smoothed fit of the data to get an overall representation of it.

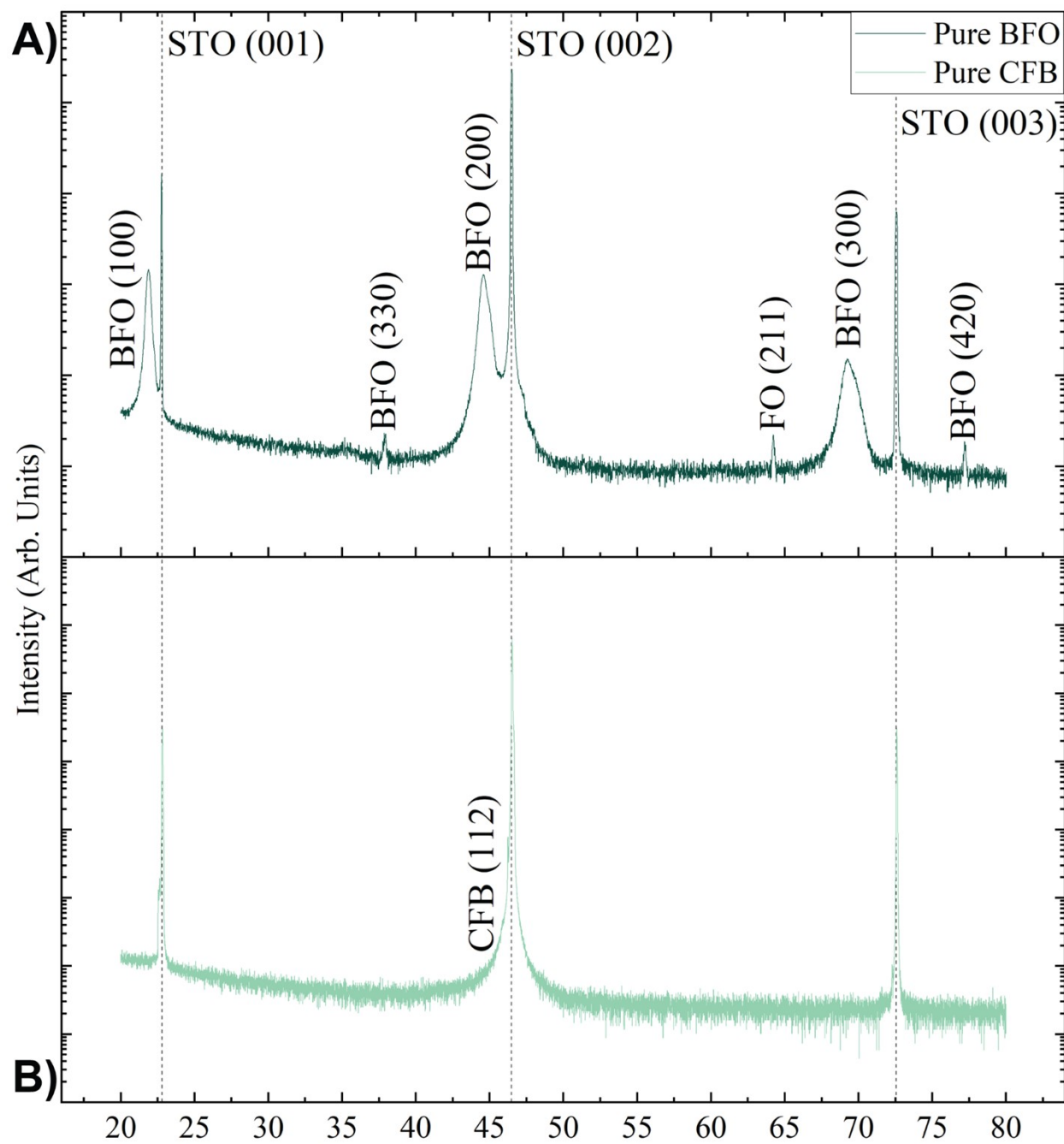


Figure S2: XRD  $\theta$ - $2\theta$  of the A) Pure CFB film and B) Pure BFO film.

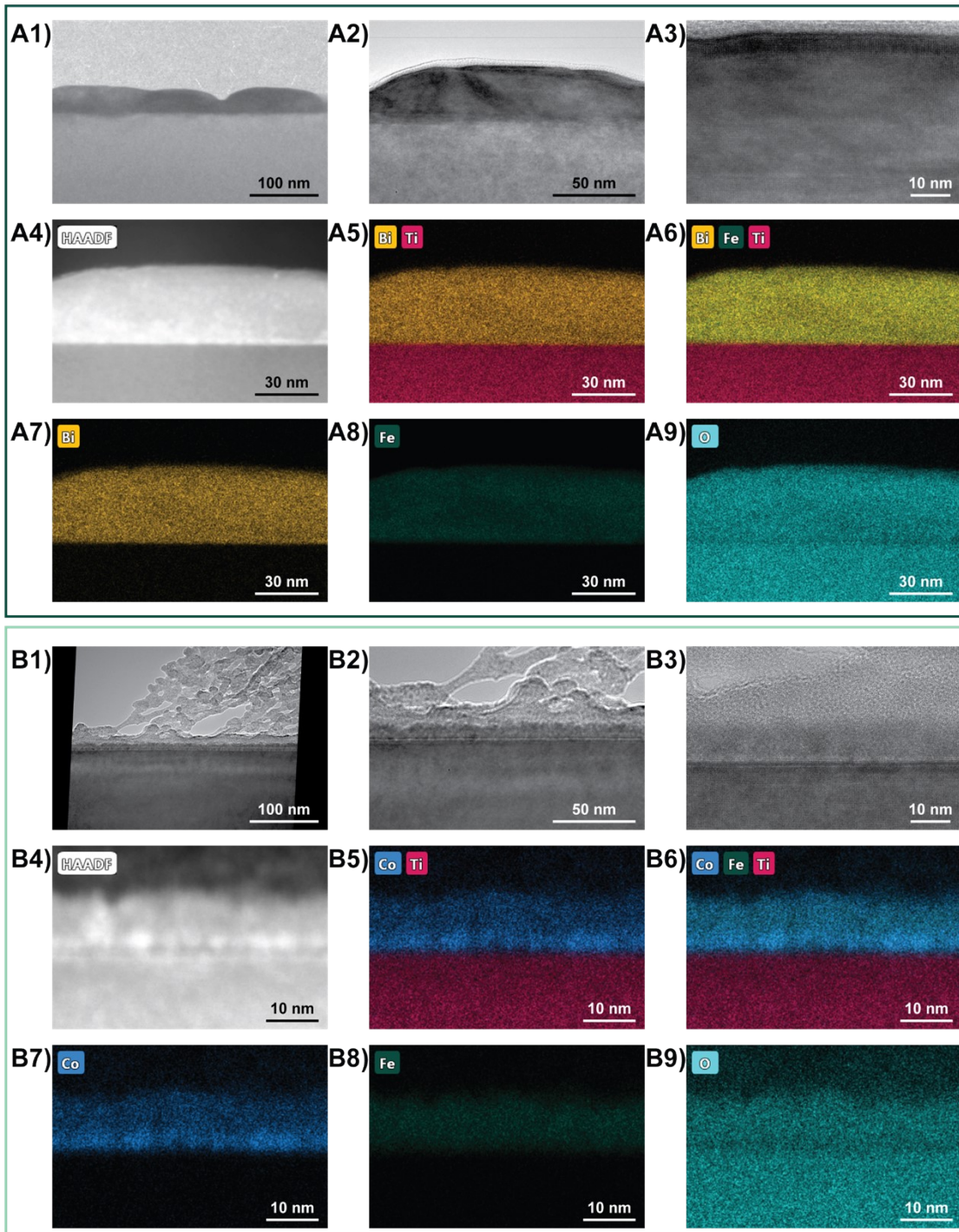


Figure S3: For the Pure BFO film: A1) Low-magnification, A2) Medium-magnification, and A3) High-magnification TEM images, A4) STEM image for the corresponding EDS maps, EDS maps of the following elements A5) Bi- and Ti-, A6) Bi-, Fe-, and Ti-, A7) Bi-, A8) Fe-, and A9) O-. For the Pure CFB film: A1) Low-magnification, A2) Medium-magnification, and A3) High-magnification TEM images, A4) STEM image for the corresponding EDS maps, EDS maps of the following elements A5) Co- and Ti-, A6) Co-, Fe-, and Ti-, A7) Bi-, A8) Fe-, and A9) O-.

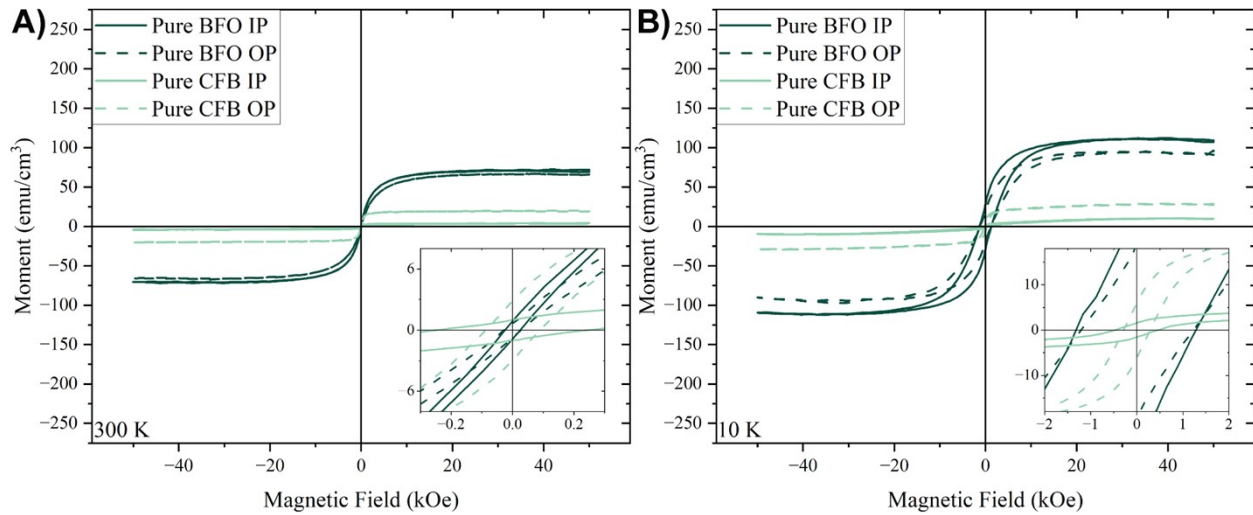


Figure S4: Magnetic hysteresis (MvsH) data showing both in-plane (IP) and out-of-plane (OP) orientations for the Pure BFO and Pure CFB films at A) 300 K and B) 10 K.

The films were deposited using pulsed laser deposition (PLD) with a KrF excimer laser (Lambda Physik,  $\lambda=248$  nm). The Pure CoFeB film was deposited at 400°C, an atmosphere of 50 mTorr N<sub>2</sub>, a laser energy of 450 mJ, laser frequency of 10 Hz, and 5000 pulses. The Pure BiFeO<sub>3</sub> film was deposited at 700°C, a 100 mTorr O<sub>2</sub> atmosphere, laser energy of 450 mJ, laser frequency of 5 Hz, and 3000 pulses. Both films were cooled to room temperature after deposition at 15°C/minute in the same atmosphere as the deposition. All films were deposited on SrTiO<sub>3</sub> (STO) substrates for XRD, TEM, and magnetic hysteresis measurements.

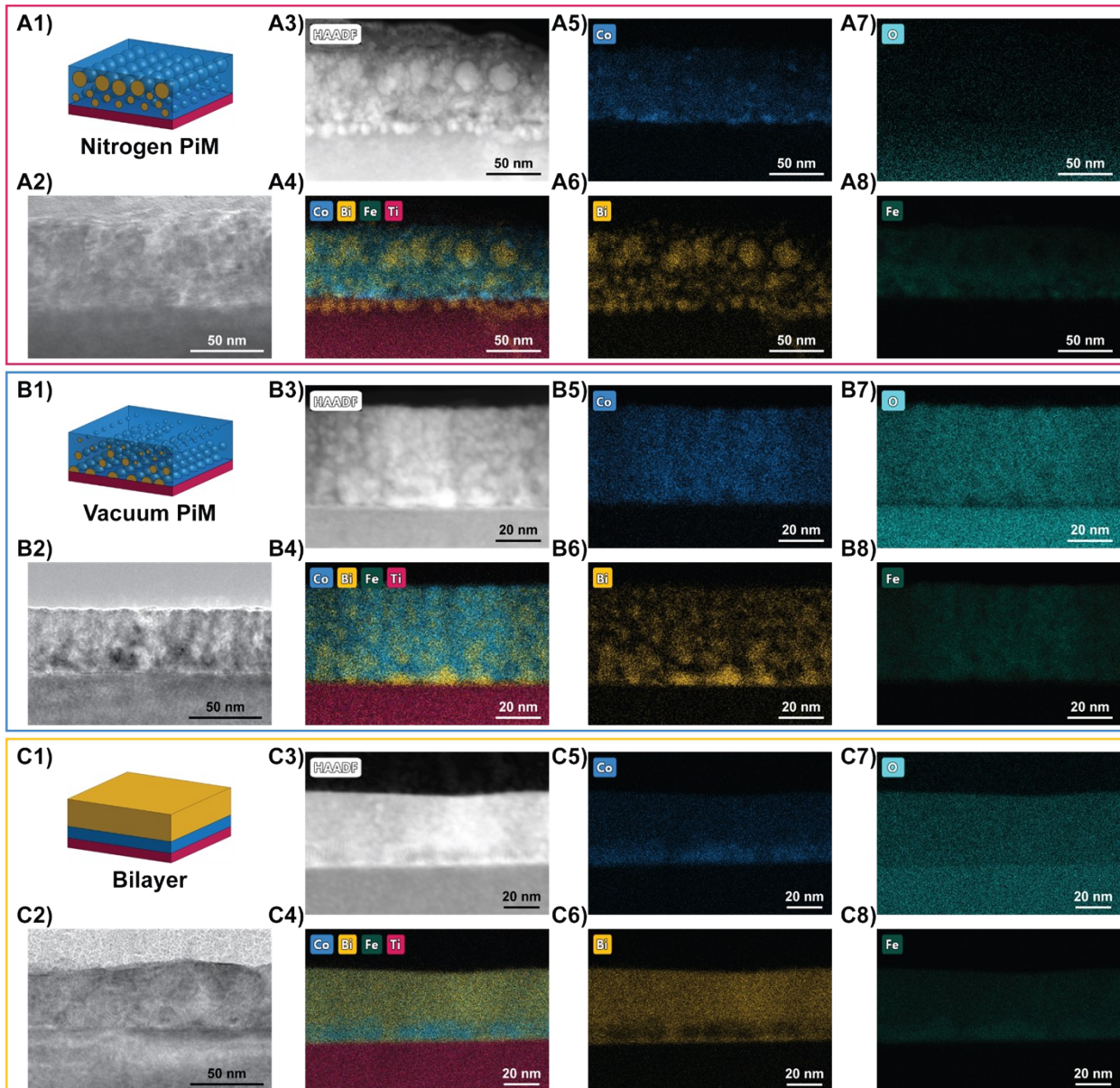


Figure S5: For the Nitrogen PiM film: A1) Schematic drawing, A2) Medium-magnification TEM image, A3) STEM image for corresponding EDS maps, EDS maps of the following elements A4) Co-, Bi-, Fe-, and Ti-, A5) Co-, A6) Bi-, A7) O-, and A8) Fe-. For the Vacuum PiM film: B1) Schematic drawing, B2) Medium-magnification TEM image, B3) STEM image for corresponding EDS maps, EDS maps of the following elements B4) Co-, Bi-, Fe-, and Ti-, B5) Co-, B6) Bi-, B7) O-, and B8) Fe-. For the Bilayer film: C1) Schematic drawing, C2) Medium-magnification TEM image, C3) STEM image for corresponding EDS maps, EDS maps of the following elements C4) Co-, Bi-, Fe-, and Ti-, C5) Co-, C6) Bi-, C7) O-, and C8) Fe-.

Table S1: List of Film Thicknesses

	Film Thickness (nm)
Nitrogen PiM	74.08
Vacuum PiM	41.18
Bilayer	45.98
Pure BFO	32.51
Pure CFB	11.67

Table S2: List of the Saturation Magnetization and Coercivity for all the samples.

		300 K		10 K	
		Saturation (emu/cm <sup>3</sup> )	Coercivity (kOe)	Saturation (emu/cm <sup>3</sup> )	Coercivity (kOe)
Nitrogen PiM	IP	181.38	0.2820	211.70	7.75
	OP	188.63	0.5724	221.13	8.24
Vacuum PiM	IP	176.72	0.5809	228.47	7.39
	OP	189.97	1.62	243.63	8.98
Bilayer	IP	51.80	0.5291	68.35	12.19
	OP	56.87	0.9874	69.12	12.15
Pure BFO	IP	70.71	0.0248	109.04	1.30
	OP	65.79	0.0282	91.63	1.22
Pure CFB	IP	3.87	0.2470	9.87	0.4729
	OP	20.03	0.0885	28.82	0.2910

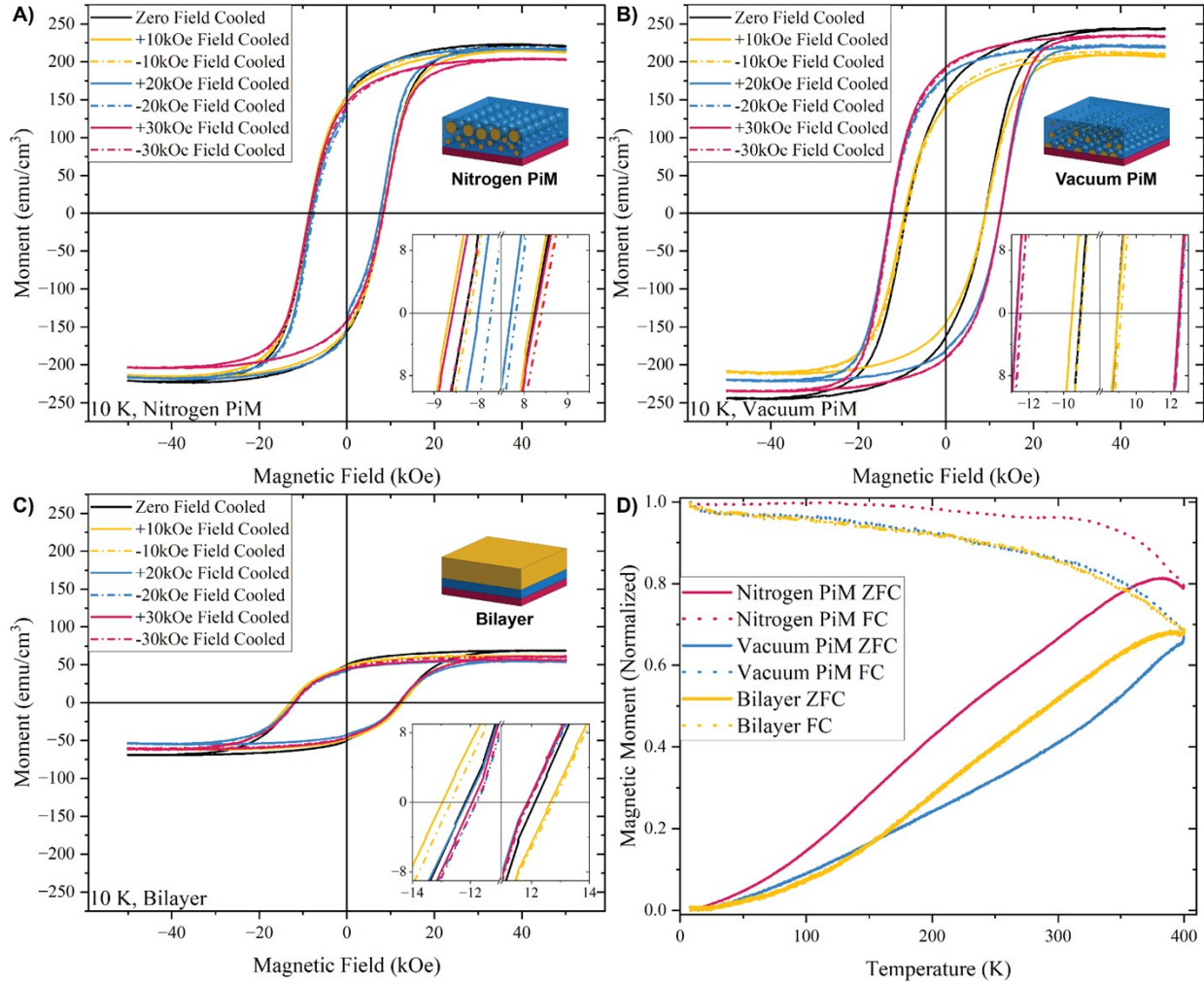


Figure S6: Magnetic hysteresis ( $M$  vs.  $H$ ) data showing the out-of-plane data at 10 K after Zero-Field Cooling, Positive Field Cooling, and Negative Field Cooling for the A) Nitrogen PiM film, B) Vacuum PiM film, and C) Bilayer Film. D) Normalized Zero Field-Cooled (ZFC) and Field-Cooled (FC) for the Nitrogen PiM, Vacuum PiM, and Bilayer films. The measurement was done with an applied field of 1000 Oe, and the normalization was done individually for each sample.

Table S3: List of the Average Coercive Field,  $H_C$ , (kOe), Exchange Bias Field,  $H_{EB}$ , (kOe), and Average Saturation Magnetization,  $M_S$ , (emu/cm<sup>3</sup>) of the Nitrogen PiM, Vacuum PiM, and Bilayer films after cooling to 10 K under Zero-Field, applied positive fields, and applied negative fields..

		Nitrogen PiM	Vacuum PiM	Bilayer
-30 kOe Applied Cooling Field	$H_C$	8.34	12.50	11.87
	$H_{EB}$	0.12	0.06	0.13
	$M_S$	203.11	234.18	60.07
-20 kOe Applied Cooling Field	$H_C$	7.65	12.53	11.84
	$H_{EB}$	0.16	0.05	0.12
	$M_S$	217.12	220.43	54.27
-10 kOe Applied Cooling Field	$H_C$	8.29	9.06	12.71
	$H_{EB}$	0.20	0.19	0.08
	$M_S$	215.66	210.33	61.14
0 kOe Applied Cooling Field	$H_C$	8.27	8.98	12.15
	$H_{EB}$	-0.03	-0.07	-0.05
	$M_S$	220.96	243.90	69.08
+10 kOe Applied Cooling Field	$H_C$	8.42	9.23	12.82
	$H_{EB}$	-0.47	-0.56	-0.31
	$M_S$	213.21	207.95	60.60
+20 kOe Applied Cooling Field	$H_C$	7.77	12.61	12.00
	$H_{EB}$	-0.40	-0.20	-0.28
	$M_S$	215.97	219.63	53.59
+30 kOe Applied Cooling Field	$H_C$	8.42	12.58	11.90
	$H_{EB}$	-0.30	-0.21	-0.08
	$M_S$	203.42	233.93	58.78

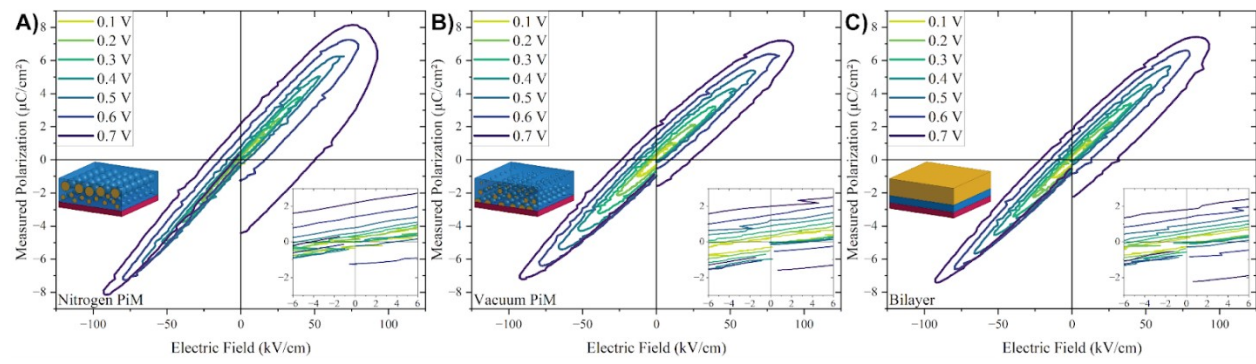


Figure S7: Electrical hysteresis ( $P$  vs.  $E$ ) data for the A) Nitrogen PiM, B) Vacuum PiM, and C) Bilayer films.

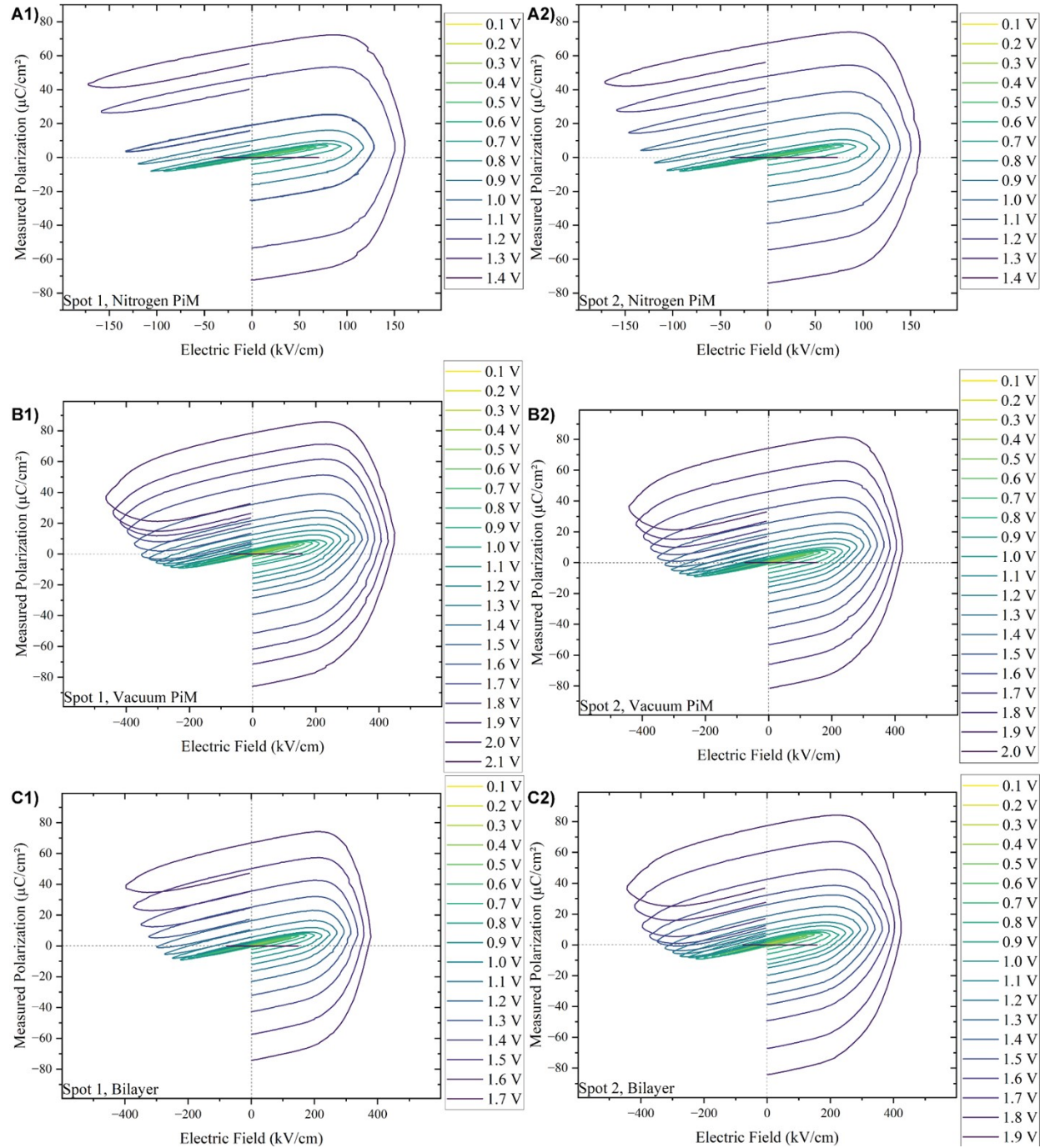


Figure S8: Electrical hysteresis ( $P$  vs.  $E$ ) data for the Nitrogen PiM sample at A1) First measured spot, A2) Second measured spot, for the Vacuum PiM film B1) First measured spot, B2) Second measured spot, and for the Bilayer film C1) First measured spot, C2) Second measured spot.